Supplementary Information (SI) for Dalton Transactions.

Supporting Information

Enhancement in the performance of $Nb_{14}W_3O_{44}$ high power anodes through P doping in the tetrahedral sites

A. J. Green*[ab], J. W. Annis[ab], D. J. Gardner[ab], A. Spiller[a], P. K. Allan[ab] and P. R. Slater*[ab]

** Corresponding authors*

a School of Chemistry, University of Birmingham, Edgbaston, Birmingham, B15 2TT, UK.

b The Faraday Institution, Harwell Campus, Didcot, OX11 0RA, UK.

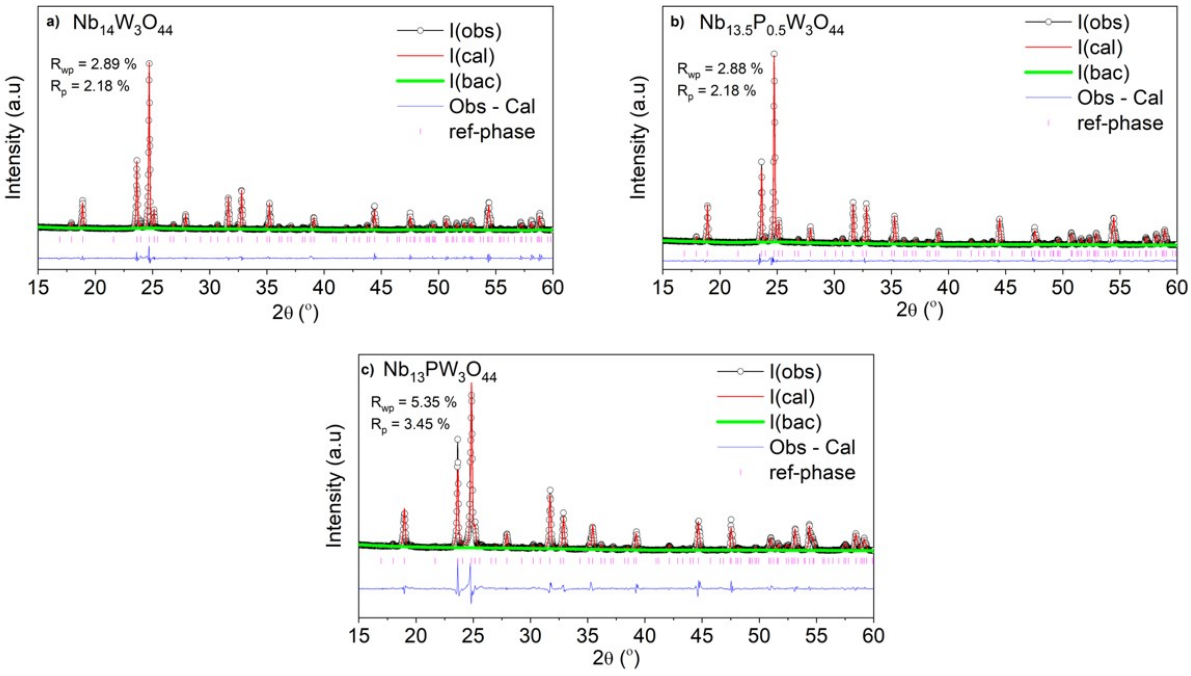

SI Figure 1: Observed, calculated and difference XRD profiles for a) $Nb_{14}W_3O_{44}$ (Rwp – 2.89 %, Rp – 2.18 %), b) $Nb_{13.5}P_{0.5}W_3O_{44}$ (Rwp – 2.88 %, Rp – 2.18 %), and $Nb_{13}PW_3O_{44}$ (Rwp – 5.35 %, Rp – 3.45 %). c) (Cu Kα) from Rietveld refinement.

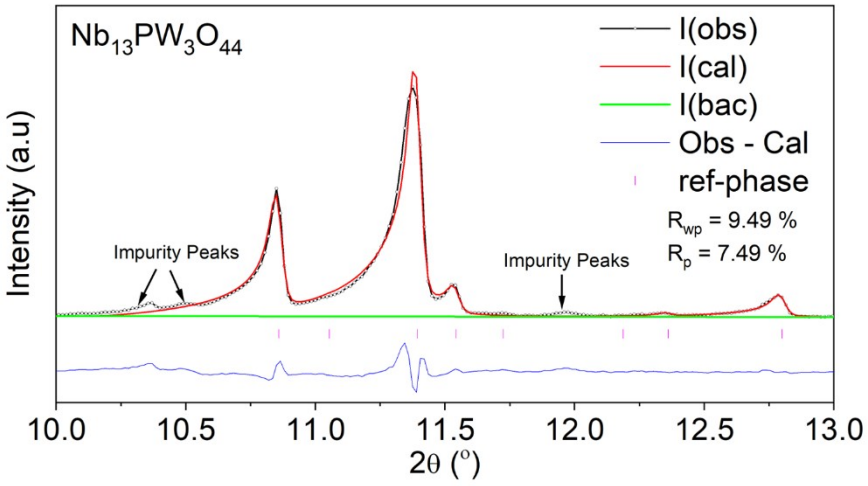

SI Figure 2: Observed, calculated and difference XRD profile for $Nb_{13}PW_3O_{44}$ capillary scan zoomed in between 10-13° 2θ. The extra peaks from the impurity phase are highlighted with arrows.

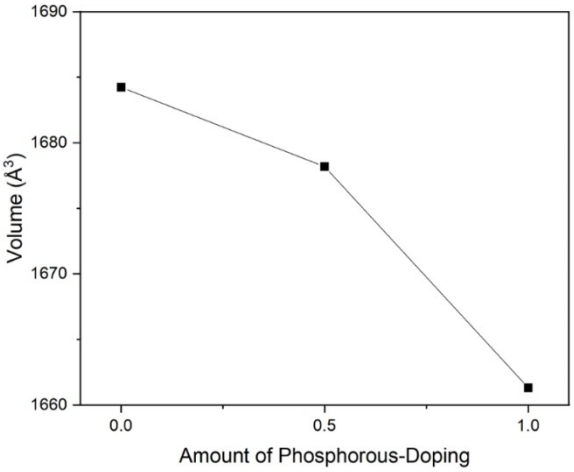

SI Figure 3: Variation of unit cell volume of $Nb_{14-x}P_xW_3O_{44}$ vs. phosphorous-content.

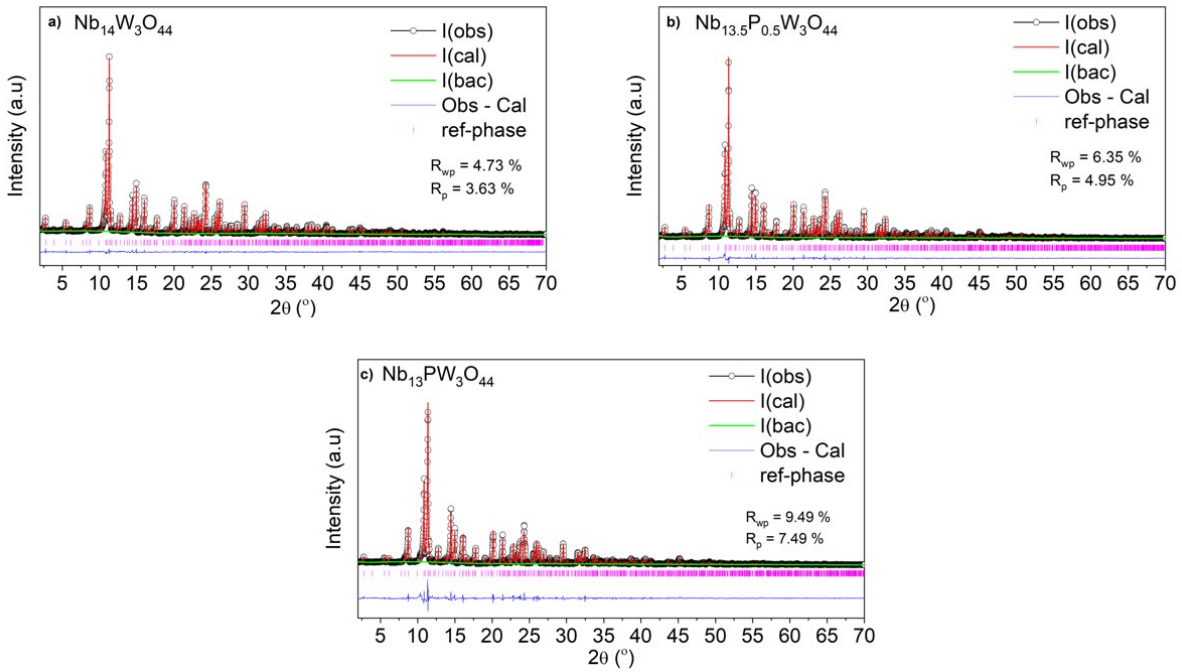

SI Figure 4: Observed, calculated and difference XRD profiles for a) $Nb_{14}W_3O_{44}$ (Rwp – 4.73 %, Rp – 3.63 %), b) $Nb_{13.5}P_{0.5}W_3O_{44}$ (Rwp – 6.35 %, Rp – 4.95 %), and c) $Nb_{13}PW_3O_{44}$ (Rwp – 9.49 %, Rp – 7.49 %). (Mo Kα) from Rietveld refinement.

SI Table 1: Refined structural parameters for $Nb_{14}W_3O_{44}$.

Label	Multiplicity	x	y	z	Fraction	U_{iso}
W1	4	0.0	0.5	0.25	0.497(5)	0.0096(4)
Nb1	4	0.0	0.5	0.25	0.00	0.0096(4)
W2	8	0.4459(2)	0.2160(2)	0.0	0.05(1)	0.008(1)
W3	8	0.1233(2)	0.0356(2)	0.5	0.223(9)	0.0199(8)
W4	8	0.2120(2)	0.1950(2)	0.5	0.06(1)	0.009(1)
W5	8	0.3721(2)	0.1064(2)	0.5	0.07(1)	0.007(1)
Nb2	8	0.4459(2)	0.2160(2)	0.0	0.95(1)	0.008(1)
Nb3	8	0.1233(2)	0.0356(2)	0.5	0.777(9)	0.0199(8)
Nb4	8	0.2120(2)	0.1950(2)	0.5	0.94(1)	0.009(1)
Nb5	8	0.3721(2)	0.1064(2)	0.5	0.93(1)	0.007(1)
O1	8	0.178(1)	0.120(1)	0.5	1	0.013(1)
O2	8	0.2976(9)	0.1526(9)	0.5	1	0.013(1)
O3	8	0.333(1)	0.030(1)	0.5	1	0.013(1)
O4	8	0.4675(9)	0.0624(8)	0.5	1	0.013(1)
O5	8	0.086(1)	0.956(1)	0.5	1	0.013(1)
O6	8	0.1248(9)	0.034(1)	0.0	1	0.013(1)
O7	8	0.229(1)	0.2074(8)	0.0	1	0.013(1)
O8	8	0.4371(8)	0.1810(9)	0.5	1	0.013(1)
O9	8	0.3926(9)	0.1317(9)	0.0	1	0.013(1)
O10	8	0.136(1)	0.2402(9)	0.5	1	0.013(1)
Composition					$Nb_{14.39(18)}W_{2.61(9)}O_{44}$	

SI Table 2: Refined structural parameters for $Nb_{13.5}P_{0.5}W_3O_{44}$.

Label	Multiplicity	x	y	z	Fraction	U_{iso}
P1	4	0.0	0.5	0.25	0.25	0.007(1)
W1	4	0.0	0.5	0.25	0.322(5)	0.007(1)
Nb1	4	0.0	0.5	0.25	0.0	0.007(1)
W2	8	0.4439(1)	0.2171(2)	0.0	0.08(1)	0.006(1)
W3	8	0.1229(2)	0.0343(2)	0.5	0.26(1)	0.024(1)
W4	8	0.2144(2)	0.1941(2)	0.5	0.04(1)	0.006(1)
W5	8	0.3741(2)	0.1035(2)	0.5	0.07(1)	0.013(1)
Nb2	8	0.4439(2)	0.2171(2)	0.0	0.92(1)	0.006(1)
Nb3	8	0.1229(2)	0.0344(2)	0.5	0.74(1)	0.024(1)
Nb4	8	0.2144(2)	0.1941(2)	0.5	0.96(1)	0.006(1)
Nb5	8	0.3741(2)	0.1035(2)	0.5	0.93(1)	0.013(1)
O1	8	0.177(1)	0.117(1)	0.5	1	0.011(1)
O2	8	0.295(1)	0.1554(9)	0.5	1	0.011(1)
O3	8	0.339(1)	0.029(1)	0.5	1	0.011(1)
O4	8	0.4634(9)	0.0593(9)	0.5	1	0.011(1)
O5	8	0.083(2)	0.952(1)	0.5	1	0.011(1)
O6	8	0.124(1)	0.038(1)	0.0	1	0.011(1)
O7	8	0.237(1)	0.213(1)	0.0	1	0.011(1)
O8	8	0.437(1)	0.178(1)	0.5	1	0.011(1)
O9	8	0.383(1)	0.121(1)	0.0	1	0.011(1)
O10	8	0.136(1)	0.238(1)	0.5	1	0.011(1)
O11	8	0.488(1)	0.282(1)	0.0	1	0.011(1)
Composition				$Nb_{14.20(8)}P_{0.5}W_{2.44(8)}O_{44}$		

SI Table 3: Refined structural parameters for $Nb_{13}PW_3O_{44}$.

Label	Multiplicity	x	y	z	Fraction	U_{iso}
P1	4	0.0	0.5	0.25	0.5	0.018(5)
W1	4	0.0	0.5	0.25	0.168(8)	0.018(5)
Nb1	4	0.0	0.5	0.25	0.0	0.018(5)
W2	8	0.4402(4)	0.2162(4)	0.0	0.06(2)	0.007(2)
W3	8	0.1249(3)	0.0342(3)	0.5	0.34(2)	0.022(2)
W4	8	0.2187(4)	0.1912(4)	0.5	0.02(2)	0.020(4)
W5	8	0.3774(3)	0.0995(3)	0.5	0.09(2)	0.009(3)
Nb2	8	0.4402(4)	0.2162(4)	0.0	0.94(2)	0.007(3)
Nb3	8	0.1249(3)	0.0343(3)	0.5	0.66(2)	0.022(2)
Nb4	8	0.2187(4)	0.1912(4)	0.5	0.98(2)	0.020(4)
Nb5	8	0.3774(3)	0.0995(3)	0.5	0.91(2)	0.009(3)
O1	8	0.191(1)	0.131(2)	0.5	1	0.006(2)
O2	8	0.298(1)	0.143(1)	0.5	1	0.006(2)
O3	8	0.333(1)	0.023(1)	0.5	1	0.006(2)
O4	8	0.463(1)	0.062(1)	0.5	1	0.006(2)
O5	8	0.072(1)	0.961(2)	0.5	1	0.006(2)
O6	8	0.130(2)	0.018(2)	0.0	1	0.006(2)
O7	8	0.230(2)	0.205(2)	0.0	1	0.006(2)
O8	8	0.440(2)	0.186(2)	0.5	1	0.006(2)
O9	8	0.390(2)	0.125(2)	0.0	1	0.006(2)
O10	8	0.147(2)	0.244(2)	0.5	1	0.006(2)
O11	8	0.492(2)	0.280(2)	0.0	1	0.006(2)
Composition					$Nb_{13.96(16)}PW_{2.38(16)}O_{44}$	

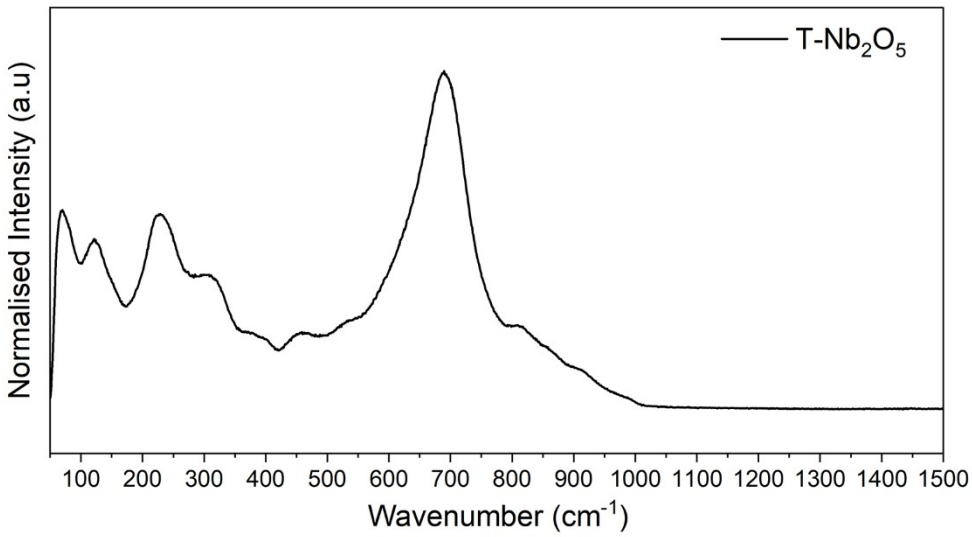

SI Figure 5: Raman spectrum of T-Nb_2O_5.

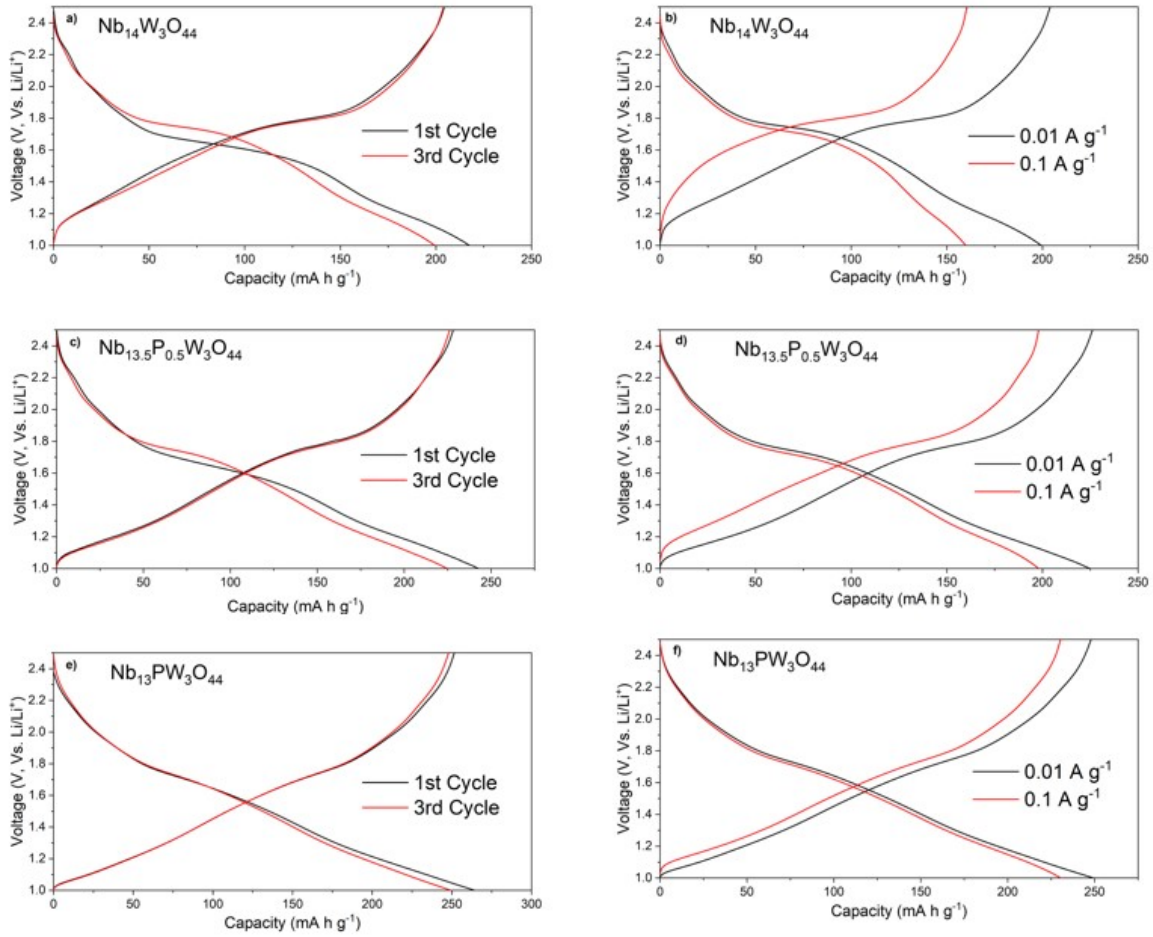

SI Figure 6: The figures on the left are galvanostatic charge-discharge curves for the 1st and 3rd formation cycles of $Nb_{14}W_3O_{44}$ (a), $Nb_{13.5}P_{0.5}W_3O_{44}$ (c), and $Nb_{13}PW_3O_{44}$ (e), vs. Li metal at a rate corresponding to 0.01 A g^{-1}. The figures on the right are galvanostatic charge-discharge curves comparing the 3rd formation cycle at 0.01 A g^{-1} against the 1st cycle at 0.1 A g^{-1}for $Nb_{14}W_3O_{44}$ (b), $Nb_{13.5}P_{0.5}W_3O_{44}$ (d), and $Nb_{13}PW_3O_{44}$ (f), vs. Li metal.

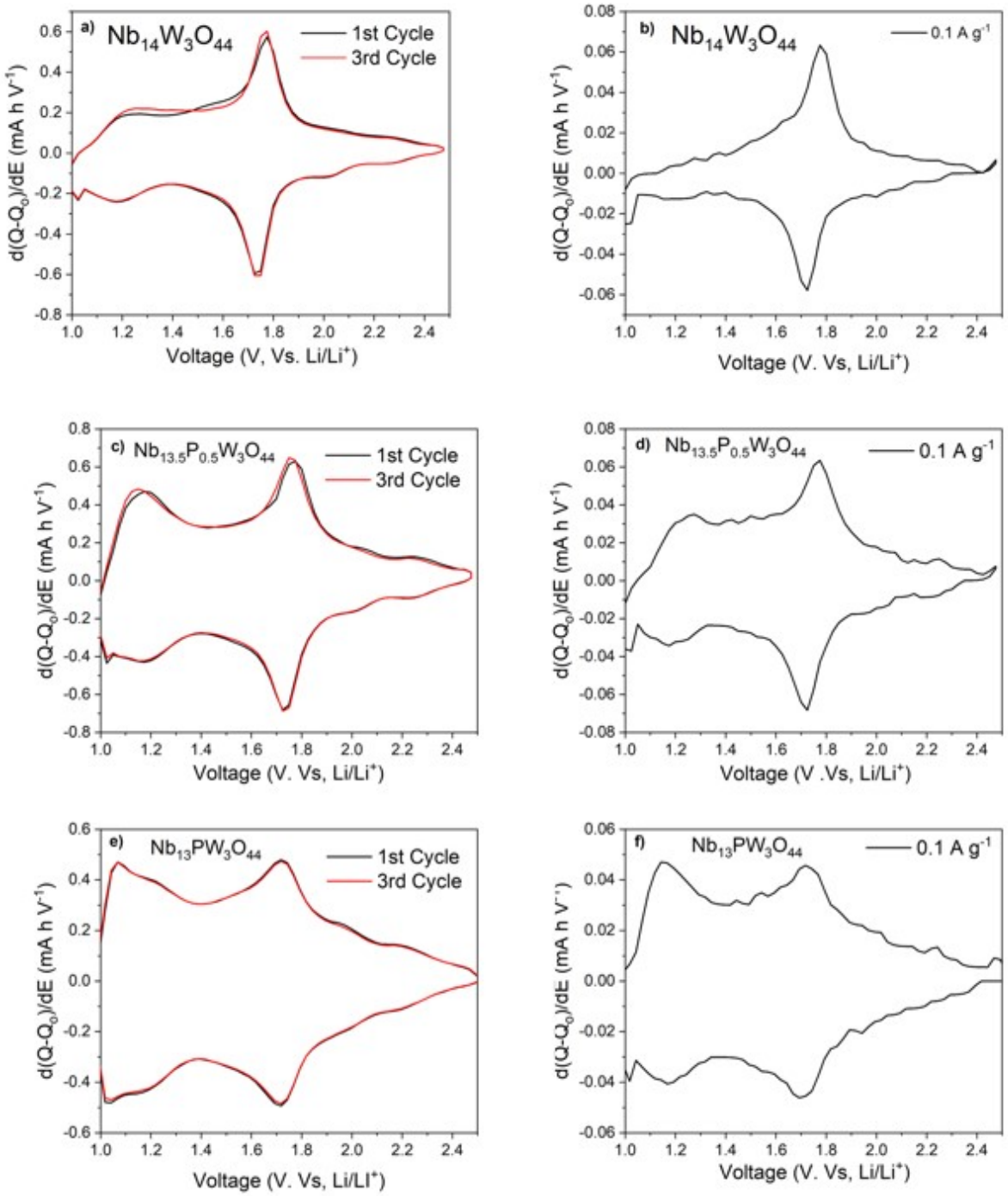

SI Figure 7: The figures on the left are differential scanning calorimetry (dQ/dV) plots derived from the galvanostatic discharge/charge profile of the 1st and 3rd formation cycles of $Nb_{14}W_3O_{44}$ (a), $Nb_{13.5}P_{0.5}W_3O_{44}$ (c), and $Nb_{13}PW_3O_{44}$ (e), vs. Li metal at a rate corresponding to 0.01 A g^{-1}. The figures on the right are differential scanning calorimetry (dQ/dV) plots derived from the galvanostatic discharge/charge profile for the 1st cycle at 0.1 A g^{-1} for $Nb_{14}W_3O_{44}$ (b), $Nb_{13.5}P_{0.5}W_3O_{44}$ (d), and $Nb_{13}PW_3O_{44}$ (f), vs. Li metal.

SI Table 4: The corresponding capacity and calculated moles of Li intercalated for $Nb_{14-x}P_xW_3O_{44}$ for the first and third formation cycles for x=0, 0.5, 1.0.

X = 0			**x = 0.5**			**x = 1**		
Cycle	**Capacity (mA h g^{-1})**	**Li^+**	**Cycle**	**Capacity (mA h g^{-1})**	**Li^+**	**Cycle**	**Capacity (mA h g^{-1})**	**Li^+**
1st	217	21.0	1st	246	23.2	1st	251	23.4
3rd	206	19.6	3rd	231	21.8	3rd	244	22.7
Li^+ Difference		1.4	**Li^+ Difference**		1.4	**Li^+ Difference**		0.7